

1 **Application of the LM-BP neural network approach for**
2 **landslide risk assessments**

3 Junnan Xiong^{1,3,*}, Ming Sun², Hao Zhang¹, Weiming Cheng³, Yinghui Yang¹,
4 Mingyuan Sun¹, Yifan Cao¹ and Jiyan Wang¹

5 ¹School of Civil Engineering and Architecture, Southwest Petroleum University, Chengdu, 610500,
6 P.R. China

7 ²Geodetic Third Team, National Administration of Surveying, Mapping and Geo-information of China,
8 Chengdu, 610100, P.R. China

9 ³State Key Laboratory of Resources and Environmental Information System, Institute of Geographic
10 Science and Natural Resources Research, Chinese Academy of Sciences, Beijing 100101, P.R. China

11 *Correspondence to:* Junnan Xiong (neu_xjn@163.com)

12 Running Title: Landslide risk zonation in pipeline areas

13

Abstract. Landslide disaster is one of the main risks involved with the operation of long-distance oil and gas pipelines. Because previously established disaster risk models are too subjective, this paper presents a quantitative model for regional risk assessment through an analysis of the laws of historical landslide disasters along oil and gas pipelines. Using the Guangyuan section of the Lanzhou-Chengdu-Chongqing (LCC) Long-Distance Products Oil Pipeline (82km) in China as a case study, we successively carried out two independent assessments: a susceptibility assessment and a vulnerability assessment. We used an entropy weight method to establish a system for the vulnerability assessment, whereas a Levenberg Marquardt- Back Propagation (LM-BP) neural network model was used to conduct the susceptibility assessment. The risk assessment was carried out on the basis of two assessments. The first, the system of the vulnerability assessment, considered the pipeline position and the angle between the pipe and the landslide (pipeline laying environmental factors). We also used an interpolation theory to generate the standard sample matrix of the LM-BP neural network. Accordingly, a landslide susceptibility risk zoning map was obtained based on susceptibility and vulnerability assessment. The results showed that about 70% of the slopes were in high-susceptibility areas with a comparatively high landslide possibility and that the southern section of the oil pipeline in the study area was in danger. These results can be used as a guide for preventing and reducing regional hazards, establishing safe routes for both existing and new pipelines and safely operating pipelines in the Guangyuan section and other segments of the LCC oil pipeline.

Keywords: pipeline, landslide, risk, vulnerability, susceptibility, neural network

1. Introduction

By the year 2020, the total mileage of long-distance oil and gas pipelines is expected to exceed 160,000 km in China. This represents a major upsurge in the mileage of multinational long-distance oil and gas pipelines (Huo, Wang, Cao, Wang, & Bureau, 2016). The rapid development of pipelines is associated with significant geological hazards, especially landslides, which increasingly threaten the safe operation of pipelines (P. Wang et al., 2012; Yun & Kang, 2014; Zheng, Zhang, Liu, & Wu, 2012). Landslide disasters cause great harm to infrastructure and human life. Moreover, the wide impact area of landslides restricts the economic development of landslide-prone areas (Ding, Heiser, Hübner, & Fuchs, 2016; Hong, Pradhan, Xu, & Bui, 2015). A devastating landslide can lead to casualties, property losses, environmental damage and long-term service disruptions caused by massive oil and gas leakages (G. Li, Zhang, Li, Ke, & Wu, 2016; Zheng et al., 2012). Generally, pipeline failure or destruction caused by landslides is much more deleterious than the landslides themselves, which makes it important to research the risk assessment of geological landslide hazards in pipeline areas (Inaudi & Glisic, 2006; Mansour, Morgenstern, & Martin, 2011).

Natural disaster risk comprises a combination of natural and social attributes (Atta-Ur-Rahman & Shaw, 2015). The United Nations Department of Humanitarian Affairs expresses natural disaster risk as a product of susceptibility and vulnerability (Rafiq & Blaschke, 2012; Sari, Innaqa, & Safrilah, 2017). In recent years, progress in geographic information systems (GIS) and remote sensing (RS) technologies

have greatly enhanced our ability to evaluate the potential risks that landslides pose to pipelines (Akgun, Kınca, & Pradhan, 2012; B. Li & Gao, 2015; Sari et al., 2017). The disaster risk assessment model has been widely recognized and applied by experts and scholars all over the world. Landslide risk assessment can take the form of a qualitative (T. H. Wu, Tang, & Einstein, 1996), quantitative (Ho, Leroi, & Roberds, 2000) or semi-quantitative assessment (Yingchun Liu, Shi, Lu, Xiao, & Wu, 2015) according to actual demand. Quantitative methods and models that have been proposed for the assessment can be divided into methods of statistical analysis (Sari et al., 2017), mathematical models (Akgun et al., 2012) and machine learning (He & Fu, 2009). However, most of these methods are subjective, such as expert evaluations, analytical hierarchy processes, logistic regressions and fuzzy integration methods, which could affect the accuracy and reasonableness of the evaluation (Fall, Azzam, & Noubactep, 2006; Sarkar & Gupta, 2005). This shortcoming can be overcome through the artificial neural network, especially the mature Back Propagation (BP) Neural Network that is widely used in function approximation and pattern recognition (Ke & Li, 2014a; P. L. Li, Tian, & Li, 2013; Su & Deng, 2003). The evaluation indicator system generally includes disaster characteristics, disaster prevention and pipeline attributes (Jianfeng Li, 2010; Shuiping Li, 2008). The fault tree analysis, fuzzy comprehensive evaluation and the grey theory are used to evaluate the failure probability of the system through indicator weight and scoring (Shi, 2011; Ye, Jiang, Yao, Xia, & Zhao, 2013). In previous studies, pipeline vulnerability evaluation indicators only considered the pipeline itself, and the relationship between the pipeline and environment was rarely examined (W. Feng, Zhang, & Zhang, 2014; Shuiping Li, 2008; Yingchun Liu et al., 2015). In this paper, the interaction between landslide hazards and the pipeline itself was considered, which improved the quantitative degree of the evaluation.

Based on the theory of the LM-BP neural network, a standard sample matrix was developed using the interpolation theory after an analysis of the distribution characteristics of landslides that occurred in the study area was performed and a regional landslide susceptibility assessment was completed. Considering the interaction between landslide disasters and the pipeline itself, the pipeline vulnerability evaluation in the landslide area was realized using the entropy weight method. This paper established a risk assessment model and methods for assessing landslide geological susceptibility of oil pipelines by comprehensively utilizing GIS and RS technology, which together improved the quantitative degree of the assessment.

2. Study Area

The study area was Guangyuan City in the Sichuan province, which was further restricted to the area from 105°15' to 106°04' E and 32°03' to 32°45' N, straddling 19 townships in five counties from south to north (Figure 1). The Lanzhou-Chengdu-Chongqing (LCC) Products Oil Pipeline is China's first long-distance pipeline. It begins in Lanzhou City and runs through the Shanxi and Sichuan provinces (Hao & Liu, 2008). Our study area covered sloped areas of the range with 5 km on both sides of the Guangyuan section (82 km) of the oil pipeline. The pipeline within the K558-K642 mileages may be affected by the slope areas. The Guangyuan section, located in northern Sichuan, is a transitional zone from the basin to the mountain. It features a terrain of moderate and low mountains, crisscrossed networks of ravines and a strong fluvial incision. Altitudes in this area range from 328 m to 1505 m. The study area has a subtropical monsoon climate with four distinctive seasons and annual precipitation measuring about 900

mm to 1,000 mm. Moreover, two large unstable faults (the Central Fault of Longmen Mountain and Longmen Mountain's Piedmont Fault Zone) make the area geologically unstable and prone to frequent geological hazards (Shiyuan Li et al., 2012). Guangyuan, through which the pipeline passes, has a high incidence of landslides, some of which have happened 300 times in the Lizhou and Chaotian districts (Y. Zhang, Shi, Gan, & Liu, 2011). In this area, landslide geological hazards seriously threaten the safe operation of the LCC oil pipeline.

3. Data Sources

Landslide susceptibility assessment, pipeline vulnerability assessment and geological hazard risk assessment of the landslide pipeline were made successively. Digital elevation model (DEM) data with 30 m accuracy was sourced from the Geospatial Data Cloud (<http://www.gscloud.cn/>). Precipitation data was downloaded from the dataset of annual surface observation values in China between the years 1981 to 2010, as published by the China Meteorological Administration (<http://data.cma.cn/>). This data was collected from 18 meteorological observatories near and within the study area and interpolated using the kriging method (at a resolution of 30 m × 30 m). Geological maps and landslide data (historical landslides) in the study area were obtained from the Sichuan province's geological environmental monitoring station. RS images (GF-1, multispectral 8 m, resolution 2 m) were provided by the Sichuan Remote Sensing Center.

The location of the middle line of the pipeline was detected through the direct connection method (i.e., the transmitter's output line was directly connected to the metal pipeline) using an RD8000 underground pipeline detector. Pipeline midline coordinates were measured using total network Real Time Kinematic technology, and simultaneously, the coordinates of the pipe ancillary facilities (including test piles, mileage piles and milestones) were acquired. Mileage data obtained through inner pipeline detection was derived from the China Petroleum Pipeline Company.

4. Methods

4.1 Assessment unit

Division precision and the scale of the slope unit (i.e., the basic element for a regional landslide susceptibility assessment) were in keeping with the results of the evaluation (Qiu, Niu, ZhaoYannan, & Wu, 2015). A total of 315 slope units were divided using hydrologic analysis in ArcGIS (v. 10.4) (Fig. 2a). The irrational unit was artificially identified and modified by comparing GF-1 satellite remote sensing images. Boundary correction, fragment combination and fissure filling were used for modification.

The object of the pipeline vulnerability assessment in the landslide area was the pipeline. Considering both previous research and the particulars of the research object, we used a comprehensive segmentation method based on GIS to divide the pipelines in our study. A total of 180 pipes were divided in the study area, of which the longest was about 1.7 km, and the shortest was only about 10 m (Fig. 2b).

4.2 Assessment indicators

Based on selection principles of the indicator system and the formation mechanism of landslide geological hazards, as few indicators as possible were selected to reflect the degree of danger posed by the landslide as accurately as possible (Avalon Cullen, Al-Suhili, & Khanbilvardi, 2016; Jaiswal, Westen, & Jetten, 2010; Ray, Dimri, Lakhera, & Sati, 2007). The internal factors in these indicators of the paper included topography, geological structure, stratigraphic lithology and surface coverage. Similarly, the external factors included mean annual precipitation (MAP) and the coefficient of the variation of annual rainfall (CVAR). The correlations between indicators were analyzed using R (v. 3.3.1), and the results showed a significant correlation between MAP and CVAR ($R = 0.99$) and between NDWI and NDVI ($R = 0.87$). Based on correlation and standard deviation, CVAR and NDWI were eliminated from the original evaluation system for landslide susceptibility assessment in the pipeline area (Table 1).

Generally, the evaluation indicator of pipeline vulnerability as it relates to the relationship between a pipeline and its surrounding environment is rarely considered. The evaluation indicators in this paper were refined to include pipeline parameters and the spatial relationship between a pipeline and landslide. The pipelines in the study area were based in mountainous areas and had been running for many years. All of these pipelines consisted of high-pressure pipes that were made of steel tubes and had a diameter of 610 mm for conveying oil. In keeping with the theory of the entropy weight method, these indicators (e.g., pressure, materials, diameter and media) were not included in the final evaluation system used to determine pipeline vulnerability.

4.3 LM-BP neural network Model

The neural network, an abstract model of our brain, constructs calculating units connecting with one another. Neural network has an input layer, a hidden layer and an output layer. With its good performance on nonlinear statistical modeling, it is very useful in exploring the hidden relationships between the inputs and the outputs (Z. Wu & Wang, 2016). BP Neural network with many adjustable parameters has powerful parallel processing mechanism, high flexibility and is good at dealing with a lot of uncertain information. The mechanism of landslide evaluation is complex, with many uncertainties and incomplete information (Jie et al., 2015). The BP neural network model can find out the intrinsic rules from the vast amount of complex and fuzzy data in the changing environment and make corresponding inferences. This method can be applied to the landslide susceptibility assessment of pipeline area with more qualitative information and less quantitative information, and the more accurate assessment results can be obtained from the analysis of these fuzzy information. Landslide susceptibility assessment is essentially a study of pattern recognition (F. Feng, Wu, Niu, Xu, & Yu, 2017). BP neural network can approximate arbitrary continuous function with arbitrary precision, so it is widely used in non-linear modeling, pattern recognition and pattern classification (Xiong, Ran, Xiong, Li, & Ye, 2010). Because the BP neural network model is widely used, there are many successful cases for reference in the number of neurons in each layer, the parameters of network learning and the optimization of algorithms, which can effectively improve the reliability and accuracy of the model (Ke & Li, 2014b).

The LM algorithm, also known as the damped least square method, has the advantage of local fast convergence. Its strong global searching ability contributes to the strong extrapolation ability of the trained network. LM algorithm is a combination of gradient descent method and Gauss-Newton

method. Its iteration process is no longer along a single negative gradient direction, which greatly improves the convergence speed and generalization ability of the network (Jing Li, Feng, Wang, & Zhang, 2016). The BP neural network model, optimized by the LM algorithm, was used to evaluate the regional landslide susceptibility in this study. MATLAB 2014 with the *trainlm* training function was used to implement the LM-BP neural network. The flow chart of LM-BP neural network algorithm is shown in Figure 3.

Data from 106 landslide disasters was collected near the research area. Of these landslides, 23 were within the region of the study area. Most of the landslides located outside the study area were less than 20 km away from the pipeline. Due to comparable environmental conditions, these landslides could still help us identify the relationship between landslides and environment factors. In light of the frequency distribution of each evaluation indicator (Fig. 4), the landslide susceptibility grade corresponding to each interval of the indicators was divided, and then the susceptibility degree monotonicity in each interval was decided. For this study, the landslide susceptibility grade was divided into four levels: low (I), medium (II), high (III) and extremely high (IV). Based on previous research experience and field investigations (Appendix 8), the monotonous intervals of different indicators of susceptibility degrees were judged (Appendix 1). For instance, there were hardly any landslides, only collapses that occurred in slopes above 60 degrees. Besides, the susceptibility degree in the area was monotone decreasing in the interval of [60, 90]. Because of the very small sliding force in a slope at 0 degrees to 15 degrees, landslides were rare to occur here, even under other extreme conditions. (Q. Zhang, Xu, Wu, & Li, 2015). On the basis of the classification criteria of the evaluation indicators used to predict landslide susceptibility degree and the functional relationship between the evaluation indicators and landslide probabilities, standard samples (training samples and test samples) were built using a certain mathematical method. According to the order of susceptibility from low to high, Interpolation was performed in each interval and the sample vectors of each evaluation indicator were constructed. Each 200 is a susceptibility level, and the sample vector length of each evaluation indicator is 800. The interval of the susceptibility degree is [0, 1], and the output vector is obtained by interpolating 800 values equidistantly between the interval of [0, 1]. Sample matrix is built by interpolation theory, which avoids the excess human influence in the process of building neural network model by traditional methods. The training samples and test samples were evaluated using similar construction methods but with different sample sizes. Finally, the indicator data was normalized, it was entered into the LM-BP neural network for simulation and 315 slope unit landslide susceptibility values were output.

4.4 Vulnerability assessment model for pipelines

The vulnerability evaluation model of pipelines in the landslide area was established using the entropy weight method, which overcame the shortcomings of the traditional weight method that does not consider the different evaluation indicators and the excessive human influence on the process of evaluation (Gao, Li, Wang, Li, & Lin, 2017; Pal, 2014). Entropy is a method of measuring the uncertainty of information by using probability theory (P. Liu & Zhang, 2011). The entropy indicates the extent of difference in an indicator, and the more difference of the data, the greater the role in evaluation (Jia, Zhao, Nan, & Zhao, 2007). The extremum difference method was used to normalize each indicator value. The decision

information of each index can be expressed by entropy value e_i :

$$r_{ij} = \frac{x_{ij} - \min_j \{x_{ij}\}}{\max_j \{x_{ij}\} - \min_j \{x_{ij}\}}, \quad r_{ij} = \frac{\max_j \{x_{ij}\} - x_{ij}}{\max_j \{x_{ij}\} - \min_j \{x_{ij}\}} \quad (1)$$

$$e_i = \frac{\sum_{j=1}^n p(x_{ij}) \ln p(x_{ij})}{\ln(n)} \quad (2)$$

$$p(x_{ij}) = \frac{r_{ij}}{\sum_{j=1}^n r_{ij}} \quad (3)$$

$$w_i = \frac{1 - e_i}{m - \sum_{i=1}^m e_i} \quad (4)$$

$$H_j = \sum_{i=1}^m w_i r_{ij} \quad (5)$$

where n is the number of evaluation objects, and r_{ij} represents the i^{th} evaluation indicator values of j^{th} pipe sections. H_j is the evaluation value of the pipeline section's vulnerability; w_i is the weight of the evaluation indicator;

Pipeline defect density was obtained from the pipeline internal inspection data, which consisted of both mileage data that needed to be converted into three-dimensional coordinate data and pipeline center line coordinate data obtained through C# programming. In addition, the main slide direction of the landslide was replaced by the slope direction that was extracted by DEM. The coordinate azimuth of the pipe section was extracted using the linear vector data of each pipe section, and the angle between the pipeline and the slope was calculated using the mathematical method. The calculation process was solved in the VB language on ArcGIS using second development functions. Finally, the entropy weight of 5 indicators was calculated by programming in MATLAB 2014. The entropy weight calculation results for pipeline landslide vulnerability assessment are shown in Table 2.

5 Results and Comparison

5.1 Regional landslide susceptibility assessment

The LM-BP neural network was trained and the network was stopped after 182 iterations. An RMSE value of 9.93e-09 indicated that the goal of precision had been reached. Through the simulation of the network test, none of the absolute error values of test data (20 groups) were found to be greater than 0.02; this result aligned with our expectation of the precision of the landslide susceptibility assessment. The landslide susceptibility grade was divided into four levels by using the equal interval method at intervals of 0.25. The safe section (low susceptibility) was located in the central part of the study area. The dangerous (high susceptibility) section was located north and south (Fig. 5). In the study area, most of the exposed rock was dominated by shale, which belonged to the easy-slip rock group.

Average altitude ranged from 450 m to 1400 m, and the relative height difference was greater than 80 m, with the slope between 15 ° and 35 °. Based on an overlay analysis of historic landslides within the study area, and susceptibility zonation maps, we surmised that the probability of landslides in the study area was extremely high, and that 87% of the landslides occurred in the medium-, high-, and extremely high-susceptibility areas. Among these landslides, three were located in low-susceptibility areas, which accounted for 13% of the landslide disaster sites, five occurred in medium-susceptibility areas (accounting for 21.7% of disaster sites), seven occurred in high-susceptibility areas (accounting for 30.4% of sites) and eight occurred in extremely high-susceptibility areas (accounting for 34.8% of sites). The evaluation results were found to accurately reflect the trends and rules of distribution of landslides in the study area. The number and area of slopes in high-susceptibility and extremely high-susceptibility areas accounted for about 70% of the total (Table 3). The probability of landslide occurrence in the study area was generally high, which was consistent with the fact that the region was landslide-prone.

5.2 Vulnerability assessment for oil pipeline in landslide area

The equal interval of 0.25 was used to divide the pipeline vulnerability level into four grades to obtain the pipeline vulnerability zonation of the study area (Fig. 6). The pipeline in the northern part of the study area was given a low vulnerability grade, while the situation in the south of the region is more serious. The number, length and percentage of pipeline segments with different grade vulnerabilities are shown in Table 4. The number and length of pipeline segments in highly vulnerable areas (III) and extremely vulnerable areas (IV) accounted for about 12% of the total.

5.3 Risk assessment for oil pipeline in landslide area

According to natural disaster risk expressions released by the UN, the definition of risk may be expressed as the product of landslide susceptibility in a pipeline area and pipeline vulnerabilities in the landslide area. **Scientific analysis and expression of disaster risk assessment results can simplify complex risk assessment and make the micro results macro (Ding & Tian, 2013). There is no unified criterion for disaster evaluation zoning, and the equal interval method is one of the methods to express the results more intuitively (H. Hu, Dong, & Pan, 2011; Jin & Meng, 2011; Y. Wang, Hao, Zhao, & Fang, 2011). The susceptibility degrees and vulnerability degrees were distinguished using the equal interval method, and four risk grades were then automatically generated.** Where the comprehensive risk assessment value was within 0 to 0.0625, the corresponding risk grade was Grade I; the corresponding risk grades with the values of 0.0625 to 0.25, 0.25 to 0.5625 and 0.5625 to 1.0 were Grade II, III and IV, respectively. The risk grade of each section of the pipeline within the research area is shown in Fig. 7.

The number of sections with a high-risk grade was 33, which accounted for 18.33% of all pipeline sections and represented 16.57% of the total pipeline length of 13.461 km). There were 4 sections with extremely high-risk grade, which accounted for 2.22% of all sections and represented 3.31% of the total pipeline length of 2.538 km. The section number and length of pipelines lying in high-risk (III) and extremely high-risk (IV) areas accounted for 20% of the total pipeline length, and the risk grade of pipelines inside Qingchuan and Jian'ge County was relatively high.

5.4 Analysis of risk assessment results

Large or huge landslides were common in areas that we categorized as extremely high risk, which we defined as those that were geologically evolving or had experienced obvious deformations within the last 2 years with still visible cracks. These pipelines were subject to dangers at any time, as the pipelines within the areas prone to landslides were found to contain many defects or extensive damage. These areas also posed considerable threats; for example, pipeline ruptures or breaks could lead to leakages or serious deformations that cause transportation failure. Because these are unacceptable events, risk prevention and control measures must be taken in a short time. Pipelines with extremely high risk were mainly distributed in the following areas: (1) Xiasi Village in Xiasi County (Pile No. K628-K630); (2) Shiweng Village-Maliu Village of Xiasi County (Pile No. K635-K637). This section lay in the south of the research area, with an altitude of 500 m to 750 m. Here, the slope conditions affected the distribution of groundwater pore pressure and the physical and mechanical characteristics of the rock and soil in three areas: vegetation cover, evaporation and slope erosion. Ultimately, these three factors affected slope stability (Luo & Tan, 2011). Vertical and horizontal ravines have also been seen in this section, with a relative height difference greater than 100 m and slope between 15 ° to 35 °. Slope degrees with obvious changes had a great influence on slope stability (Chang & Kim, 2004; W. Hu, Xu, Wang, Asch, & Hicher, 2015). The exposed rocks in this area were mainly shale and belonged to the sliding-prone rock group. Rock type and interlayer structure were found to be important internal indicators that a landslide could occur (Guzzetti, Cardinali, & Reichenbach, 1996; Xiang et al., 2010; Xin, Chong, & Dai, 2009). The distance between the fault and the pipeline in the section was about 2 km with a NDVI of about 0.75 and MAP of about 970 mm. Faulted zones and nearby rock and earth masses that were destroyed in a geologic event reduced the integrity of a slope, and the faults and important groundwater channels could also cause deformation and damage of a slope (Yinghui Liu, 2009). The pipelines in these areas exhibited many defects. Most pipelines passed through the slope in an inclined or horizontal way, an attribute that typically increased the risk of a landslide occurring.

In high-risk areas, small or moderate landslides commonly occurred in areas that we categorized as high risk. They were in deformation, or had obvious deformation recently (within 2 years), such as obvious cracks, subsidence or tympanites on the landslide and even shear. The pipelines in these areas had defects and were buried at a shallow depth. If a landslide occurred in this pipeline area, it could cause pipe suspension, floating and damage. It could also contribute to a small to moderate leakage of the medium. However, damaged pipes can be welded or repaired. Monitoring is critical in high-risk areas. In our study, the pipeline high-risk area was defined by the following areas: (1) Xiasi Town Xiasi Village-Shiweng Village (pipe No. K622-K633). (2) Xiasi Town Maliu Village Jinzishan Xiangdasang Village (pipe No. K635-K642). This area was located in the south of the pipe, which was buried in the study area. The altitude of the study area was between 450 m and 800 m, the relative elevation difference was over 100m and the slope was between 15 ° and 40 °. Most of the outcrops in this area were quartz sandstone, which belonged to the easy-sliding rock group. The pipes in this area were about 2.5 km away from faults. The NDVI was about 0.6 to 0.8, and MAP was about 970 nm. Pipes showed many defects, most of them either crossing the slope or lying in the center of slope. All of the above factors provided sufficient conditions for the formation of landslide.

In the medium-risk areas, only small landslides were found to occur, and we observed no sign of

deformation. But through the analysis of geological structure, topography and landform, we found the area to demonstrate a tendency for developing landslides. The pipes in this risk area exhibited almost no faults and were buried deep beneath the ground. However, under bad conditions, the landslides in these areas could also affect the pipes' safety, causing the pipes to become exposed or deformed. These areas need simple monitoring. For our study, medium-risk areas were defined as follows: (1) Sanlong village of Dongxihe township-Panlong town Dongsheng village (pipe No. K559-K593). (2) Panlong town Qinlao village-Wu'ai village (pipe No. K595-K597). (3) Baolun town Laolin'gou village-Xiasi town Youyu village (pipe No. K599-K630).

In the low-risk areas, landslides didn't occur under ordinary conditions, but they could occur if a strong earthquake hit or if the area experienced continuous or heavy rain. The pipes in low-risk areas showed no defects and were buried very deep. They were also located far away from areas affected by landslides. Therefore, landslides in these areas caused no obvious damage to the pipes, and few threatened the safety of pipes. However, regular inspection is necessary to ensure that the pipes continue to operate safely. The pipe low-risk area were defined as follows: (1) Panlong town Dongsheng village-Qinlao village (pipe No. K591-K597). (2) Baolun town Xiaojia village-Baolun town Laolin'gou village (pipe No. K599-K608).

Through comprehensive analysis of each risk level area, we compiled a list of pipeline landslide risks (Table 6). This list describes each landslide risk level in four respects: pipeline risk, landslide susceptibility, pipeline vulnerability and risk control measures.

6 Conclusion

The faults inherent to traditional landslide risk assessment include excessive human influence, failure of pipeline vulnerability assessments to consider the interaction between landslide disaster and pipeline ontology and the low quantification degree of risk assessment results.

Taking the Guangyuan section (82 km) of the LCC oil and gas pipeline as an example, we used GIS and RS technology to establish a regional landslide susceptibility assessment model based on the LM-BP neural network. We determined that there were 112 and 108 slopes in high-susceptibility and extremely high-susceptibility areas that accounted for 33.18% and 40.46% of the total area of the study area, respectively. Then, we established the model of pipeline vulnerability evaluation based on the entropy weight method by combining the pipeline body and the environmental information. The number and length of pipe segments in the highly vulnerable (III) and extremely vulnerable area (IV) accounted for about 12% of the total. Finally, based on the susceptibility assessment and the vulnerability assessment, we completed the risk assessment and risk division of the oil pipeline, thus forming a geological disaster risk assessment model and a method for oil pipeline and landslide risk assessment. The risk assessment results demonstrated that the number and length of high-susceptibility and extremely high-susceptibility pipeline segments represented 20% of the total. Similarly, the pipeline risk within Qingchuan and Jian'ge Counties was relatively high. Our pipeline landslide risk assessment has laid a foundation for the future study of pipeline safety management and pipeline failure consequence loss assessment.

Acknowledgments

The study has been funded by the Strategic Priority Research Program of Chinese Academy of Sciences (XDA20030302), IWHR(China Institute of Water Resources and Hydropower Research) National Mountain Flood Disaster Investigation Project (SHZH-IWHR-57), Southwest Petroleum University Of Science And Technology Innovation Team Projects (2017CXTD09) and the Study on temporal and spatial differentiation of historical mountain flood disasters in Fujian province (NDMBD2018003).

References

- Akgun, A., Kincal, C., and Pradhan, B.: Application of remote sensing data and GIS for landslide risk assessment as an environmental threat to Izmir city (west Turkey). *Environmental Monitoring & Assessment*, 184(9), 5453-5470. [https://doi: 10.1007/s10661-011-2352-8](https://doi.org/10.1007/s10661-011-2352-8) 2012.
- Atta-Ur-Rahman, and Shaw, R. (2015). *Hazard, Vulnerability and Risk: The Pakistan Context*: Springer Japan.
- Avalon Cullen, C., Al-Suhili, R., and Khanbilvardi, R.: Guidance Index for Shallow Landslide Hazard Analysis. *Remote Sensing*, 8(10), 866. [https://doi: 10.3390/rs8100866](https://doi.org/10.3390/rs8100866), 2016.
- Chang, H., and Kim, N. K.: The evaluation and the sensitivity analysis of GIS-based landslide susceptibility models. *Geosciences Journal*, 8(4), 415-423. [https://doi: 10.1007/BF02910477](https://doi.org/10.1007/BF02910477), 2004.
- Ding, M., Heiser, M., Hübl, J., and Fuchs, S.: Regional vulnerability assessment for debris flows in China—a CWS approach. *Landslides*, 13(3), 537-550. [https://doi: 10.1007/s10346-015-0578-1](https://doi.org/10.1007/s10346-015-0578-1) 2016.
- Ding, M., and Tian, S. (2013). *Landslide and Debris Flow Risk Assessment and Its Application* Beijing: Science Press.
- Fall, M., Azzam, R., and Noubactep, C.: A multi-method approach to study the stability of natural slopes and landslide susceptibility mapping. *Engineering Geology*, 82(4), 241-263. 2006.
- Feng, F., Wu, X., Niu, R., Xu, S., and Yu, X.: Landslide susceptibility assessment based on PSO-BP neural network. *Science of Surveying* Mapping, 42(10), 170-175. [https://doi: 10.16251/j.cnki.1009-2307.2017.10.027](https://doi.org/10.16251/j.cnki.1009-2307.2017.10.027), 2017.
- Feng, W., Zhang, T., and Zhang, Y.: Evaluating the stability of landslides in xianshizhai village and the pipeline vulnerability with their action. *Journal of Geological Hazards & Environment Preservation*. 2014.
- Gao, C. L., Li, S. C., Wang, J., Li, L. P., and Lin, P.: The Risk Assessment of Tunnels Based on Grey Correlation and Entropy Weight Method. *Geotechnical & Geological Engineering*(4), 1-11. [https://doi: 10.1007/s10706-017-0415-5](https://doi.org/10.1007/s10706-017-0415-5) 2017.
- Guzzetti, F., Cardinali, M., and Reichenbach, P.: The Influence of Structural Setting and Lithology on Landslide Type and Pattern. *Environmental & Engineering Geoscience*, 2(4), 531-555. 1996.
- Hao, J., and Liu, J.: Zonation of Danger Degree of Geological Hazards over Lanzhou-Chengdu-Chongqing Products Pipeline. *Oil & Gas Storage & Transportation*. 2008.
- He, Y., and Fu, W.: Application of fuzzy support vector machine to landslide risk assessment. *Journal of Natural Disasters*, 18(5), 107-112. 2009.
- Ho, K., Leroy, E., and Roberds, B.: *Quantitative Risk Assessment : Application, Myths and Future Direction*. 2000.
- Hong, H., Pradhan, B., Xu, C., and Bui, D. T.: Spatial prediction of landslide hazard at the Yihuang area (China) using two-class kernel logistic regression, alternating decision tree and support vector machines. *Catena*, 133, 266-281. [https://doi: 10.1016/j.catena.2015.05.019](https://doi.org/10.1016/j.catena.2015.05.019) 2015.
- Hu, H., Dong, P., and Pan, j.: The Hail Risk Zoning in Beijing Integrated with the Result of Its Loss Assessment. *Journal of Applied Meteorological Science*, 22(5), 612-620. 2011.
- Hu, W., Xu, Q., Wang, G. H., Asch, T. W. J. V., and Hicher, P. Y.: Sensitivity of the initiation of debris flow to initial soil moisture. *Landslides*, 12(6), 1139-1145. [https://doi: 10.1007/s10346-014-0529-2](https://doi.org/10.1007/s10346-014-0529-2) 2015.
- Huo, F., Wang, W., Cao, Y., Wang, F., and Bureau, C. P.: China's Construction Technology of Oil and Gas Storage and Transportation and Its Future Development Direction. *Oil Forum*. 2016.
- Inaudi, D., and Glisic, B.: Reliability and field testing of distributed strain and temperature sensors. *Proceedings of SPIE - The International Society for Optical Engineering*, 6167(14), 2586–2597.

[https://doi: 10.1117/12.661088](https://doi.org/10.1117/12.661088) 2006.

Jaiswal, P., Westen, C. J. V., and Jetten, V.: Quantitative landslide hazard assessment along a transportation corridor in southern India. *Engineering Geology*, 116(3), 236-250. [https://doi: 10.1016/j.enggeo.2010.09.005](https://doi.org/10.1016/j.enggeo.2010.09.005), 2010.

Jia, Y., Zhao, J., Nan, Z., and Zhao, C.: The Application of Entropy-right Method to the Study of Ecological Security Evaluation of Grassland——A Case Study at the Ecological Security Evaluation of Grassland to Pastoral Area of Gansu. *Journal of Arid Land Resources Environmental & Engineering Geoscience*. [https://doi: 10.1016/S1872-5791\(08\)60002-0](https://doi.org/10.1016/S1872-5791(08)60002-0) 2007.

Jie, D., Yamagishi, Hiromitsu, Reza, P. H., Yunus, A. P., Xuan, S., Xu, Y., and Zhu, Z.: An integrated artificial neural network model for the landslide susceptibility assessment of Osado Island, Japan. *Natural Hazards*, 78(3), 1749-1776. 2015.

Jin, Y., and Meng, J. J.: Assessment and forecast of ecological vulnerability:A review. *Chinese Journal of Ecology*, 30(11), 2646-2652. 2011.

Ke, F., and Li, Y.: The forecasting method of landslides based on improved BP neural network. *Geotechnical Investigation & Surveying*. 2014a.

Ke, F., and Li, Y.: The forecasting method of landslides based on improved BP neural network. *Geotechnical Investigation Surveying*, 42(8), 55-60. 2014b.

Li, B., and Gao, Y. (2015). Application of the improved fuzzy analytic hierarchy process for landslide hazard assessment based on RS and GIS. Paper presented at the International Conference on Intelligent Earth Observing and Applications.

Li, G., Zhang, P., Li, Z., Ke, Z., and Wu, G.: Safety length simulation of natural gas pipeline subjected to transverse landslide. 2016.

Li, J. (2010). Wenchuan Earthquake and Secondary Geological Hazard Assessment Based on RS/GIS Technology. (Master), China University of Geosciences, Beijing, China.

Li, J., Feng, J., Wang, W., and Zhang, F.: Spatial and Temporal Changes in Solar Radiation of Northwest China Based LM-BP Neural Network. *Scientia Geographica Sinica*, 36(5), 780-786. [https://doi: 10.13249/j.cnki.sgs.2016.05.017](https://doi.org/10.13249/j.cnki.sgs.2016.05.017), 2016.

Li, P. L., Tian, W. P., and Li, J. C.: Analysis of landslide stability based on BP neural network. *Journal of Guangxi University*. 2013.

Li, S. (2008). The Risk Assessment Study on the Environmental Geological Hazards along the West-East Nature Gas Pipeline. (Mater), SouthWest JiaoTong University, Chengdu, China.

Li, S., Jian, j., Wu, Z., Li, S., Li, H., Bai, K., Ke, Q., Xu, Y., and Hu, Y.: A Design of the Geo-Environmental Management Database System for Guangyuan City *Journal of Geological Hazards and Environment Preservation*, 23(3), 7. 2012.

Liu, P., and Zhang, X.: Research on the supplier selection of a supply chain based on entropy weight and improved ELECTRE-III method. *International Journal of Production Research*, 49(3), 637-646. [https://doi: 10.1080/00207540903490171](https://doi.org/10.1080/00207540903490171), 2011.

Liu, Y. (2009). The characteristic and evaluation of collapse and landslide disaster along du-wen highway in Wenchuan earthquake region. (Master), Lanzhou University, Lanzhou.

Liu, Y., Shi, Y., Lu, Q., Xiao, H., and Wu, S.: Risk Assessment of Geological Disasters in Single Pipe Based on Scoring Index Method: A Case Study of Soil Landslide. *Natural Gas Technology & Economy*. 2015.

448 Luo, Z. F., and Tan, D. J.: Landslide Hazard Evaluation in Debris Flow Catchment Area Based on GIS
 449 and Information Method. *China Safety Science Journal*, 21(11), 144-150. [https://doi:](https://doi:10.1631/jzus.B1000265)
 450 10.1631/jzus.B1000265 2011.

451 Mansour, M. F., Morgenstern, N. R., and Martin, C. D.: Expected damage from displacement of slow-
 452 moving slides. *Landslides*, 8(1), 117-131. [https://doi: 10.1007/s10346-010-0227-7](https://doi:10.1007/s10346-010-0227-7) 2011.

453 Pal, R.: Entropy Production in Pipeline Flow of Dispersions of Water in Oil. *Entropy*, 16(8), 4648-4661.
 454 [https://doi: 10.3390/e16084648](https://doi:10.3390/e16084648) 2014.

455 Qiu, D., Niu, R., ZhaoYannan, and Wu, X.: Risk Zoning of Earthquake-Induced Landslides Based on
 456 Slope Units:A Case Study on Lushan Earthquake. *Journal of Jilin University*, 45(5), 1470-1478.
 457 [https://doi: 10.13278/j.cnki.jjuese.201505201](https://doi:10.13278/j.cnki.jjuese.201505201) 2015.

458 Rafiq, L., and Blaschke, T.: Disaster risk and vulnerability in Pakistan at a district level. *Geomatics*
 459 *Natural Hazards & Risk*, 3(4), 324-341. [https://doi: 10.1080/19475705.2011.626083](https://doi:10.1080/19475705.2011.626083) 2012.

460 Ray, P. K. C., Dimri, S., Lakhera, R. C., and Sati, S.: Fuzzy-based method for landslide hazard assessment
 461 in active seismic zone of Himalaya. *Landslides*, 4(2), 101. [https://doi: 10.1007/s10346-006-0068-6](https://doi:10.1007/s10346-006-0068-6) 2007.

462 Sari, D. A. P., Innaqa, S., and Safrilah. Hazard, Vulnerability and Capacity Mapping for Landslides Risk
 463 Analysis using Geographic Information System (GIS). 209(1), 012106. [https://doi: 10.1088/1757-](https://doi:10.1088/1757-899X/209/1/012106)
 464 899X/209/1/012106 2017.

465 Sarkar, S., and Gupta, P. K.: Techniques for Landslide Hazard Zonation – Application to Srinagar-
 466 Rudraprayag Area of Gar. *Journal of the Geological Society of India*, 65(2), 217-230. 2005.

467 Shi, S.: Risk Analysis for Pipeline Construction about Third Party Damage Based on Triangular Fuzzy
 468 Number and Fault Tree Theory. *Journal of Chongqing University of Science & Technology*. 2011.

469 Su, G., and Deng, F.: On the Improving Backpropagation Algorithms of the Neural Networks Based on
 470 MATLAB Language:A Review. *Bulletin of Science & Technology*. 2003.

471 Wang, P., Xu, Z., Bai, M., Du, Y., Mu, S., Wang, D., and Yang, Y.: Landslide Risk Assessment Expert
 472 System Along the Oil and Gas Pipeline Routes. *Advanced Materials Research*, 418-420, 1553-1559.
 473 [https://doi: 10.4028/www.scientific.net/AMR.418-420.1553](https://doi:10.4028/www.scientific.net/AMR.418-420.1553) 2012.

474 Wang, Y., Hao, J., Zhao, F., and Fang, L.: A Discussion on Regional Risk Zoning of Geological Hazard
 475 in the Worst-hit Area of the Wenchuan Earthquake in Shaanxi Province. *Journal of Catastrophology*,
 476 26(4), 35-39. [https://doi: 10.1007/s12583-011-0163-z](https://doi:10.1007/s12583-011-0163-z), 2011.

477 Wu, T. H., Tang, W. H., and Einstein, H. H. (1996). *Landslides: investigation and mitigation*. chapter 6 -
 478 landslide hazard and risk assessment.

479 Wu, Z., and Wang, H.: Super-resolution Reconstruction of SAR Image based on Non-Local Means
 480 Denoising Combined with BP Neural Network. 2016.

481 Xiang, L. Z., Cui, P., Zhang, J. Q., Huang, D. C., Fang, H., and Zhou, X. J.: Triggering factors
 482 susceptibility of earthquake-induced collapses and landslides in Wenchuan County. *Journal of Sichuan*
 483 *University*, 42(5), 105-112. 2010.

484 Xin, Y., Chong, X. U., and Dai, F. C.: Contribution of strata lithology and slope gradient to landslides
 485 triggered by Wenchuan Ms 8 earthquake,Sichuan,China. *Geological Bulletin of China*, 28(8), 1156-1162.
 486 2009.

487 Xiong, H., Ran, Y., Xiong, G., Li, S., and Ye, L.: Study on deformation prediction of landslide based on
 488 genetic algorithm and improved BP neural network. *Kybernetes the International Journal of Systems*
 489 *Cybernetics*, 39(8), 1245-1254. 2010.

490 Ye, C., Jiang, H., Yao, A., Xia, Q., and Zhao, X.: Study on risk controlling method of third party
 491 construction damage on oil and gas pipeline. *Journal of Safety Science & Technology*, 9(8), 140-145.

2013.

Yun, L., and Kang, L.: Reliability Analysis of High Pressure Buried Pipeline under Landslide. *Applied Mechanics & Materials*, 501-504, 1081-1086. [https://doi: 10.4028/www.scientific.net/AMM.501-504.1081](https://doi.org/10.4028/www.scientific.net/AMM.501-504.1081) 2014.

Zhang, Q., Xu, Q., Wu, L., and Li, J.: BP neural network model for forecasting volume of landslide group in Nanjiang. *Hydrogeology and Engineering Geology*, 42(1), 6. 2015.

Zhang, Y., Shi, J., Gan, J., and Liu, C.: Analysis of Distribution Characteristics and Influencing Factors of Secondary Geohazards in Guangyuan City——Taking Chaotian District as an Example. *Journal of Catastrophology*, 26(1), 75-79. [https://doi: 10.1007/s12182-011-0118-0](https://doi.org/10.1007/s12182-011-0118-0) 2011.

Zheng, J. Y., Zhang, B. J., Liu, P. F., and Wu, L. L.: Failure analysis and safety evaluation of buried pipeline due to deflection of landslide process. *Engineering Failure Analysis*, 25(4), 156-168. [https://doi: 10.1016/j.engfailanal.2012.05.011](https://doi.org/10.1016/j.engfailanal.2012.05.011) 2012.

505 **List of tables and figures**

506 **Table 1** Indicators of landslide susceptibility assessment and pipeline vulnerability assessment

507 **Table 2** Entropy weight of evaluation indicator

508 **Table 3** Number and area of slopes of four hazard grade

509 **Table 4** Number and distances of pipeline of four vulnerability grade

510 **Table 5** Number and distances of pipeline of four risk grade

511 **Table 6** Description of pipeline risk level

512

513 **Figure 1** Landslide location map of the study area

514 **Figure 2** All slope units (a) and pipeline section (b) in the study area

515 **Figure 3** Flow chart of LM-BP neural network algorithm

516 **Figure 4** The frequency distribution of each indicator in the landslide location. Maps (a), (b), (c), (d),
517 (e), (f), (g), and (h) represent the elevation, slope, aspect, height difference, TPC, NVI, MAP, and
518 distance from the fault, respectively

519 **Figure 5** Landslide hazard map of study area

520 **Figure 6** Pipeline vulnerability map of study area

521 **Figure 7** Pipeline risk map of study area

522

523
524
525
526
527
528
529
530
531

Table 1

Factor		Indicators
Landslide hazard indicator	Landform	Elevation
		Slope
		Aspect
		Height Difference
		Topographic profile curvature (TPC)
	Land cover	NDVI
		NDWI
	Geology	Lithology
		Distance from the fault
	Precipitation	Mean annual precipitation (MAP)
Coefficient of variation of annual rainfall (CVAR)		
Pipeline vulnerability indicator	Pipe Body	Defect Density
		Depth
		Thickness
		Pressure
		Materials
		Diameter
	Spatial relationship between pipeline and landslide	Media
		Position
		Angle

532
533

534

535

536

537

538

539

540

541

542

543

544

545

546

547

548

549

Table 2

	Depth	Angle	Defect Density	Thickness	Position
Weight	0.010007	0.101553	0.678851	0.154322	0.055266
Entropy	0.997322	0.97282	0.818308	0.958696	0.985208

550

551

552

Table 3

Landslide susceptibility	Number of slopes	Percentage (%)	Area (km ²)	Percentage (%)
Low (I)	33	10.48	32.63	8.76
Medium (II)	62	19.68	65.53	17.60
High (III)	112	35.56	123.55	33.18
Extremely high (IV)	108	34.29	150.65	40.46
Total	315	100	372.36	100

553

554

555

Table 4

Pipeline vulnerability	Number of pipelines	Percentage (%)	Area (km ²)	Percentage (%)
Low (I)	120	66.66	50.417	62.06
Medium (II)	37	20.56	20.888	25.72
High (III)	22	12.22	9.833	12.11
Extremely (IV)	1	0.56	0.087	0.11
Total	180	100	81.225	100

556

557

558

Table 5

Pipeline risk	Number of pipelines	Percentage (%)	Area (km ²)	Percentage (%)
Low (I)	37	20.56	14.469	17.81
Medium (II)	106	58.89	50.757	62.49
High (III)	33	18.33	13.461	16.57
Extremely (IV)	4	2.22	2.538	3.13
Total	180	100	81.225	100

559

560

Table 6

Pipeline risk	Landslides susceptibility	Vulnerability	Risk	Control measures
Low (I)	The landslide won't happen under ordinary conditions, but it will occur when strong earthquake, long continuous rain or extremely heavy rain happened.	The pipes in low risk areas have no any defects and buried very deep. Meanwhile, they are far away from the area affected by landslide.	Landslides have no obvious damage to the pipes, and few threats to pipes' safety.	Regular Inspection
Medium (II)	Small landslide mainly occur, and no sign of deformation. But through analyzing geological structure, topography and landform, there is a tendency of landslide.	The pipes in risk areas have almost no faults and buried deep. However, under bad condition, the landslide may also affect the pipes' safety.	The landslide may make the pipes exposed or deformation.	simple monitoring
High (III)	Landslides are most in medium-model and little-model, and they are in deformation, or have obvious deformation recently, such as obvious cracks, subsidence or tympanites on the landslide and even shear.	The pipeline has defects, and buried shallow. Once landslides occurred in the pipeline area, pipes' safety will be threatened	The safety of pipeline will be threatened and may suffer from pipe suspension, floating, and damage etc. Therefore it will contribute to a small amount of medium leakage. Fortunately, the pipe can be welded or repaired.	Main monitoring
Extremely high (IV)	Large or huge landslide is common in the area with extremely high risk, which is changing or has experienced obvious deformation recently with visible cracks.	The pipelines are subject to dangers at any time as the pipelines within the area prone to landslide have been spotted with many defects or much damage.	There are great threats, for example pipeline rupture or break and may lead to considerable leakage of media or serious deformation even transportation failure.	Prevention and control measures shall be taken in a short time

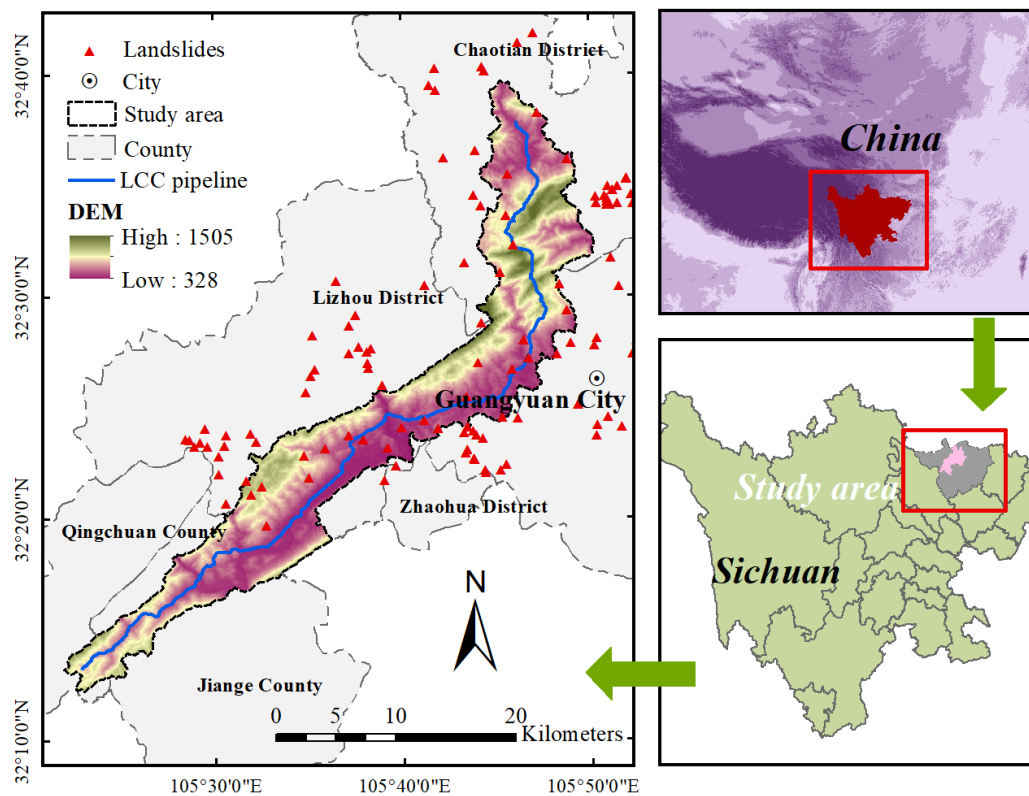


Figure 1

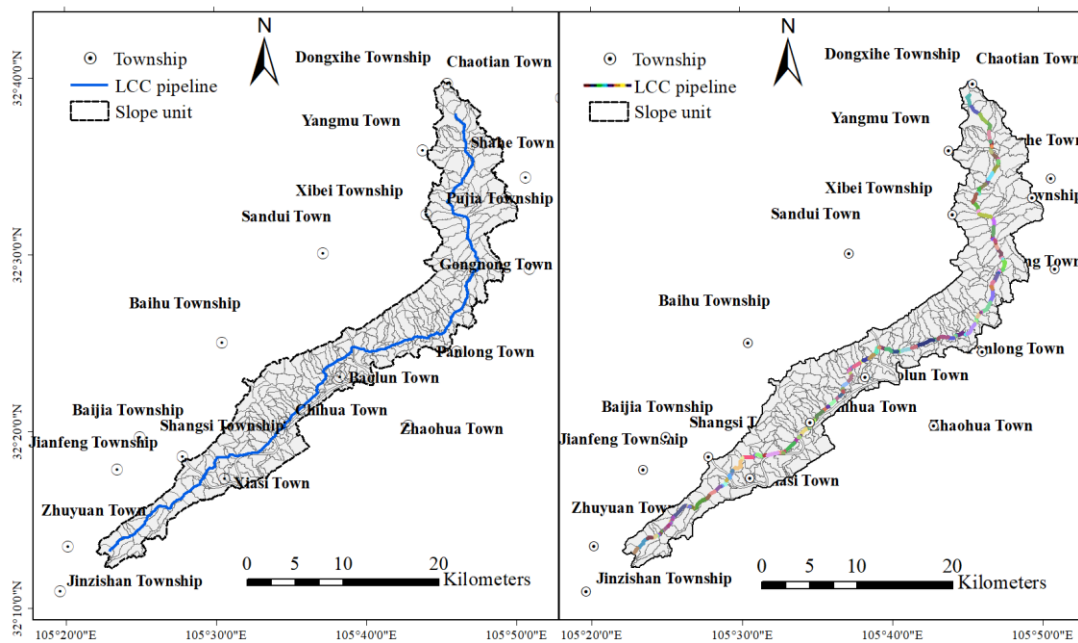


Figure 2

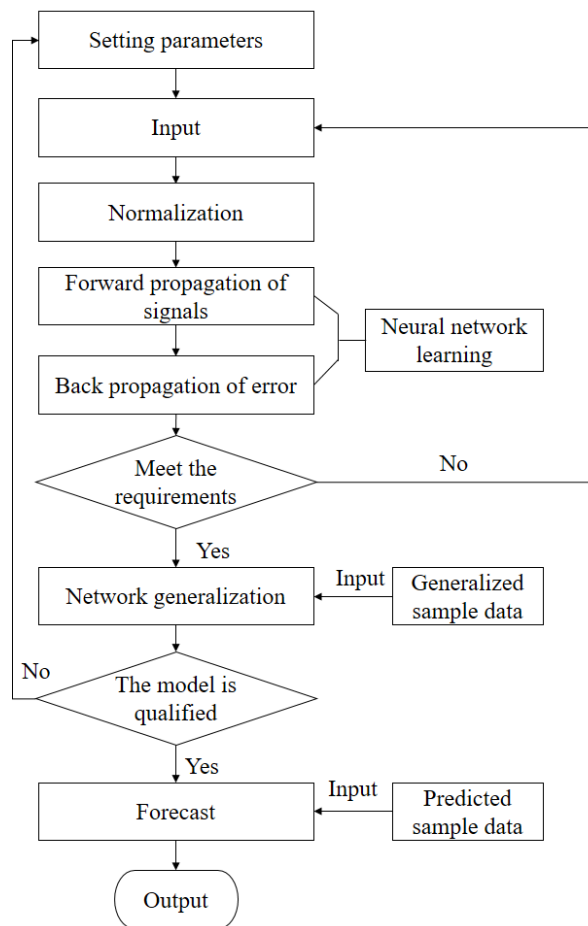


Figure 3

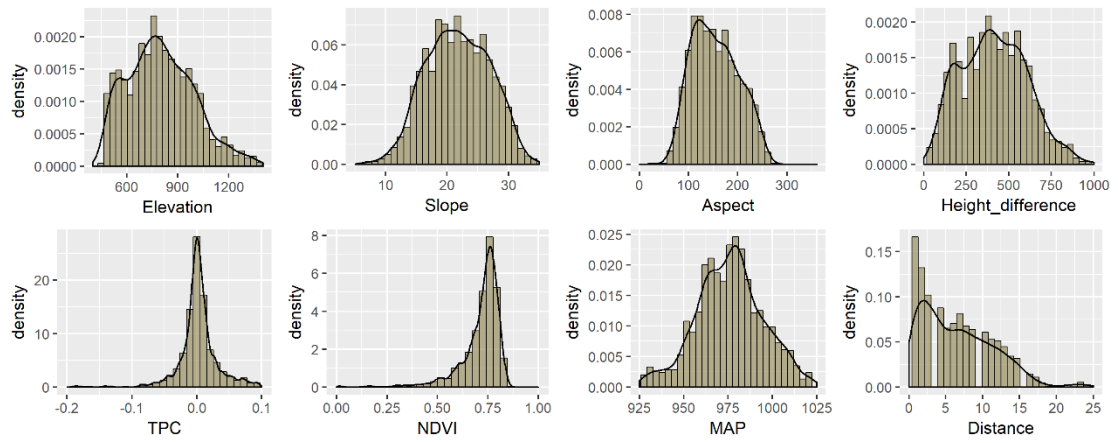


Figure 4

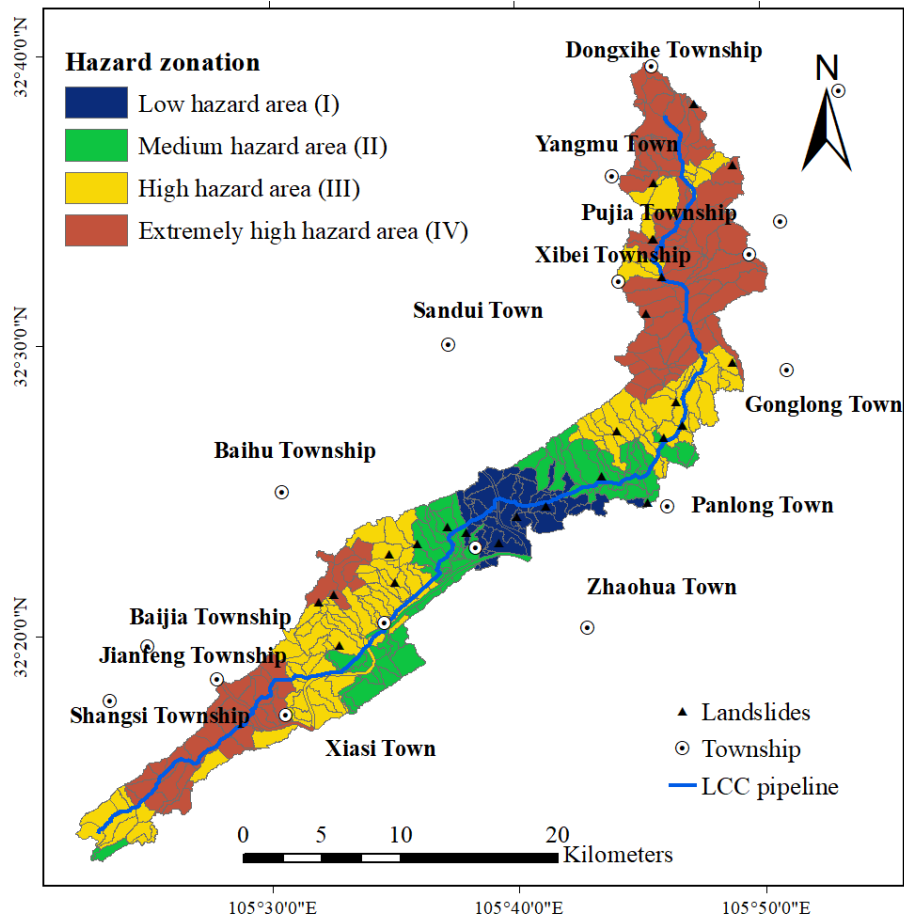


Figure 5

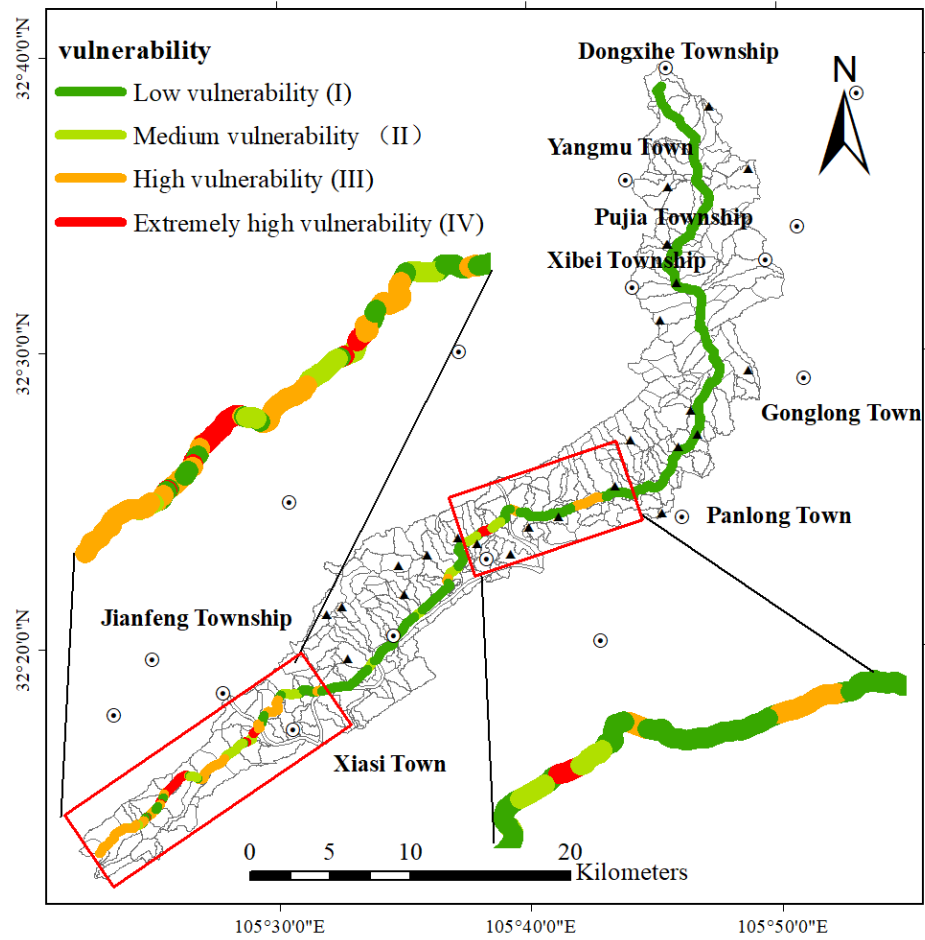


Figure 6

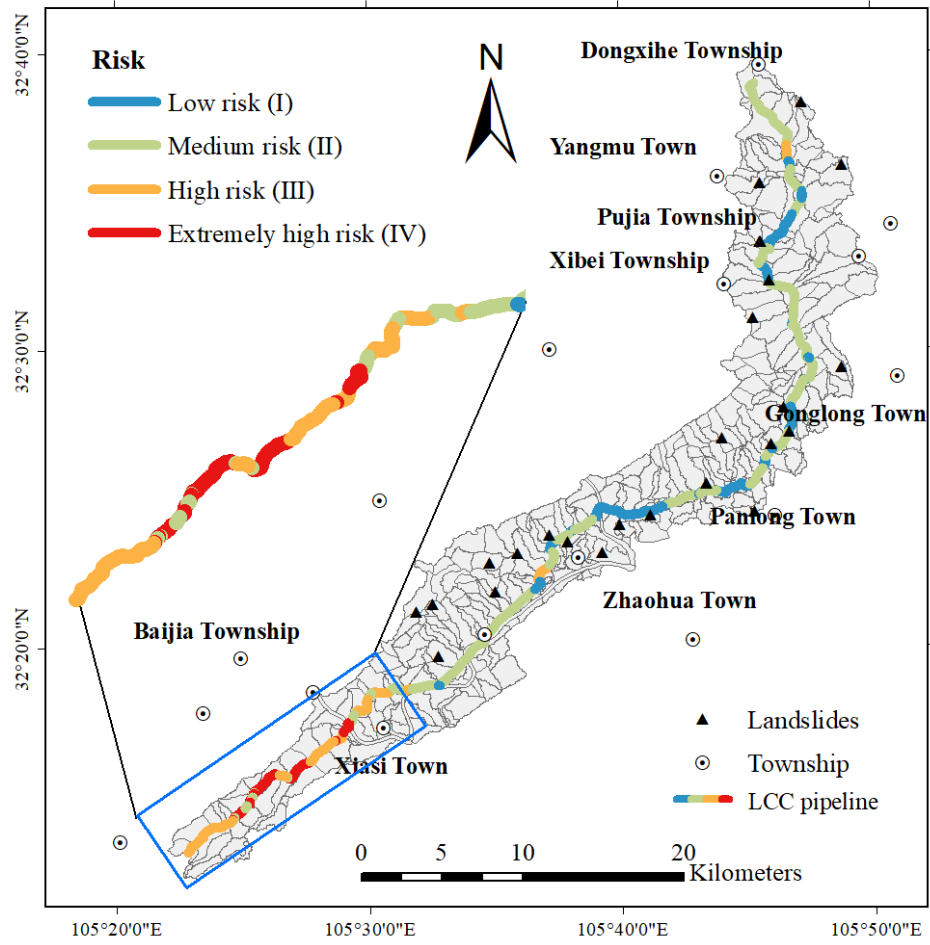


Figure 7

Appendix 1 Classification of landslide susceptibility grade corresponding to different intervals

Factor	Indicators	Interval	Susceptibility degree monotonicity	Susceptibility level
Landform	Elevation	[1000 , Highest]	Decreasing	Low susceptibility(I)
		[Lowest , 600)	Increasing	Medium susceptibility(II)
		[800 , 1000)	Decreasing	High susceptibility(III)
		[600 , 700) \cup [700 , 800)	Increasing, Decreasing	Extremely high susceptibility(IV)
	Slope	[60 , 90)	Decreasing	Low susceptibility(I)
		[0 , 15)	Increasing	Medium susceptibility(II)
		[30 , 60)	Decreasing	High susceptibility(III)
		[15 , 20) \cup [20 , 30)	Increasing, Decreasing	Extremely high susceptibility(IV)
	Aspect	[0 , 45) \cup [270 , 360)	Increasing, Decreasing	Low susceptibility(I)
		[225 , 270) \cup [45 , 90)	Decreasing, Increasing	Medium susceptibility(II)
		[90 , 135) \cup [180 , 225)	Increasing, Decreasing	High susceptibility(III)
		[135 , 157.5) \cup [157.5 , 180)	Increasing, Decreasing	Extremely high susceptibility(IV)
	Height difference	[Lowest , 100)	Increasing	Low susceptibility(I)
		[900 , Highest] \cup [100 , 200)	Decreasing, Increasing	Medium susceptibility(II)
		[600 , 900) \cup [200 , 300)	Decreasing, Increasing	High susceptibility(III)
		[300 , 450) \cup [450 , 600)	Increasing, Decreasing	Extremely high susceptibility(IV)
	topographic profile curvature	[Lowest , -0.025)	Increasing	Low susceptibility(I)
		[0.025 , Highest]	Decreasing	Medium susceptibility(II)
		[-0.025 , -0.01) \cup [0.01 , 0.025)	Increasing, Decreasing	High susceptibility(III)
		[-0.01 , 0) \cup [0 , 0.01)	Increasing, Decreasing	Extremely high susceptibility(IV)
Land cover	NDVI	[-1,0)	Increasing	Low susceptibility(I)
		[0,0.6) \cup [0.9,1]	Increasing, Decreasing	Medium susceptibility(II)
		[0.6,0.7) \cup [0.8,0.9)	Increasing, Decreasing	High susceptibility(III)
		[0.7,0.75) \cup [0.75,0.8)	Increasing, Decreasing	Extremely high susceptibility(IV)
		[1100 , Highest)	Decreasing	Low susceptibility(I)
Precipitation	Mean annual precipitation	[Lowest , 960)	Increasing	Medium susceptibility(II)
		[990 , 1100)	Decreasing	High susceptibility(III)
		[960 ,975) \cup [975 , 990)	Increasing,	Extremely high

Geology	Distance from the fault	[20, Highest]	Decreasing	susceptibility(IV)
			Decreasing	Low susceptibility(I)
		[15 , 20)	Decreasing	Medium susceptibility(II)
		[5 , 15)	Decreasing	High susceptibility(III)
		[0 ,5)	Decreasing	Extremely high susceptibility(IV)

Appendix 2 Standard training sample matrix and standard test sample matrix

Sample type	ID	Input									Output
		Aspect	Slope	Elevation	NDVI	MAP	Height Difference	TPC	Distance	Lithology	
Training sample	1	0.2	89.9	438	-1	908.1	33	-0.582	25	1	0
	50	35.2	82.8	453	0	912.2	79	-0.456	23.47	1	0.06
	100	297.1	75.7	469	0.88	916.3	115	-0.33	21.9	1	0.12
	150	329.3	67.6	485	0.95	920.4	167	-0.168	20.34	1	0.19
	200	359.5	60	499	1	924.9	200	0.628	18.77	1	0.25
	250	68.4	3.8	1293	0.73	930.4	1097	0.486	17.21	2	0.31
	300	89.3	8.2	1206	0.65	938	1039	0.326	15.64	2	0.37
	350	246	12	1102	0.56	943.6	977	0.183	14.08	2	0.44
	400	269.3	15	1002	0.5	949.8	902	-0.142	12.52	2	0.5
	450	113.4	52.9	952	0.46	960.6	848	-0.018	10.95	3	0.56
Test sample	500	134.8	46.3	905	0.4	972.6	757	-0.012	9.39	3	0.62
	1	27.2	72.3	458	0.8	911.6	59	-0.544	25	1	0
	2	28.5	71.6	468	0.81	914.3	74	-0.453	23.69	1	0.06
	3	31.5	69.5	488	0.85	915.8	86	-0.381	22.37	1	0.11
	4	37.8	66.2	490	0.86	917.1	100	-0.228	21.06	1	0.16
	5	38.6	62.1	497	0.86	919.1	152	-0.03	19.74	1	0.22
	6	56.1	4.4	1141	0.7	934.2	939	0.439	18.43	2	0.27
	7	57.3	6.6	1240	0.68	939.6	941	0.429	17.11	2	0.32
	8	65.3	9.8	1257	0.66	945.1	1124	0.413	15.79	2	0.37
	9	68.2	11	1290	0.56	948.8	1135	0.318	14.48	2	0.43
	10	74.7	11.9	1382	0.53	949.9	1146	0.148	13.16	2	0.48
	11	92.4	30.4	848	0.47	963.4	613	-0.019	11.85	3	0.53
	12	92.7	31.8	853	0.45	970.5	683	-0.016	10.53	3	0.58
	13	101.9	44.7	900	0.45	980.5	737	-0.015	9.22	3	0.64

14	110.1	50.9	917	0.35	987	817	-0.015	7.9	3	0.69
15	115.6	57.5	933	0.32	994.2	835	-0.015	6.58	3	0.74
16	140.6	15.6	502	0.14	1001.5	245	0.019	5.27	4	0.79
17	155.4	20	626	0.14	1002.3	256	0.008	3.95	4	0.85
18	157.1	24.8	690	0.08	1010.6	293	0.007	2.64	4	0.9
19	177.6	27.3	765	0.06	1012.7	392	0.004	1.32	4	0.95
20	178.3	29.6	795	0.04	1022.7	446	0.001	0	4	1

593

594

Appendix 3 Test error of LM-BP neural network

Number	Expected value	network output	error
1	0	0.0006	0.0006
2	0.06	0.0548	-0.0052
3	0.11	0.1113	0.0013
4	0.16	0.1699	0.0099
5	0.22	0.2302	0.0102
6	0.27	0.2614	-0.0086
7	0.32	0.315	-0.005
8	0.37	0.3697	-0.0003
9	0.43	0.4266	-0.0034
10	0.48	0.4899	0.0099
11	0.53	0.5153	-0.0147
12	0.58	0.5765	-0.0035
13	0.64	0.6405	0.0005
14	0.69	0.701	0.011
15	0.74	0.7523	0.0123
16	0.79	0.8094	0.0194
17	0.85	0.8616	0.0116
18	0.9	0.9155	0.0155
19	0.95	0.9675	0.0175
20	1	1.0173	0.0173

597

Appendix 4 Coordinates of the center line and ancillary facilities of the pipeline

Point number	Previous point	Material	Diameter (mm)	Pressure	Depth (m)	Coordinate			elevation
						X	Y	H	
Marker peg		--	--	--	--	..576.265	..4357.849	503.877	--
GD1.421	GD1.420	Steel	168	high	2.2	..572.111	..4352.109	504.235	502.035
GD1.422	GD1.421	Steel	168	high	1.9	..571.837	..4336.010	503.866	501.966
GD1.423	GD1.422	Steel	168	high	2.1	..571.538	..4319.679	503.694	501.594
GD1.424	GD1.423	Steel	168	high	2.1	..571.093	..4308.825	503.510	501.410
GD1.425	GD1.424	Steel	168	high	2.0	..570.718	..4288.141	503.733	501.733
Detective pole K566		--	--	--	--	..575.536	..4284.069	503.494	--
GD1.426	GD1.425	Steel	168	high	2.3	..570.603	..4275.147	503.998	501.698
Mileage peg K566+200		--	--	--	--	..574.641	..4258.41	503.224	--
GD1.427	GD1.426	Steel	168	high	2.0	..570.222	..4258.593	503.710	501.710
GD1.428	GD1.427	Steel	168	high	1.6	..570.090	..4247.642	503.283	501.683
GD1.429	GD1.428	Steel	168	high	2.3	..569.458	..4216.618	502.468	500.168
GD1.430	GD1.429	Steel	168	high	2.9	..569.043	..4208.558	504.055	501.155

598

599

600

601

602

603

604

605

606

607

Appendix 5 Internal detection data of pipeline

FID	Pipe number	distance(m)	Feature type	Remarks	Length (mm)	thickness (mm)
1	10	6.408	Pipe segment	Spiral weld	652	11.1
2	20	7.060	Pipe segment	--	1178	--
3	20	7.648	Fixed punctuation point	Valve centerline	--	--
4	20	7.650	Valve	centerline	--	--
5	30	8.238	Pipe segment	Spiral weld	768	11.1
6	40	9.006	Pipe segment	--	2184	--
7	40	10.100	Globular tee	centerline	--	--
8	50	11.190	Pipe segment	Spiral weld	1700	11.1
9	50	11.445	Pit	--	548	11.1
10	60	12.890	Pipe segment	Straight weld	2342	13.6
11	60	12.890	Wall thickness variation	from 11.1mmto 13.6mm	--	--
13	70	15.232	Pipe segment	Spiral weld	1999	11.1
14	70	15.232	Wall thickness variation	from 13.6mmto 11.1mm	--	--
15	80	17.231	Pipe segment	Straight weld	2352	13.4
16	80	17.231	Wall thickness variation	from 11.1mmto 13.4mm	--	--
18	90	19.583	Pipe segment	Spiral weld	11557	11.1
19	90	19.583	Wall thickness variation	from 13.4mmto 11.1mm	--	--
20	90	28.060	Attachments	--	598	11.1
21	100	31.140	Pipe segment	--	991	--
22	100	31.580	Flange	centerline	--	--
23	110	32.131	Pipe segment	Spiral weld	11660	11.1
24	120	43.791	Pipe segment	Spiral weld	5536	11.1
25	130	49.327	Pipe segment	Straight weld	2213	16.2
26	130	49.327	Wall thickness variation	from 11.1mmto 16.2mm	--	--

609
610
611
612
613
614
615
616

28	140	51.540	Pipe segment	Spiral weld	5608	11.1
29	140	51.540	Wall thickness variation	from 16.2mmto 11.1mm	--	--
30	150	57.148	Pipe segment	Spiral weld	9432	11.1

Appendix 6 Core Code of Pipeline Defect Point Coordinate Calculating Program

```
617
618 using System;
619 using System.Collections.Generic;
620 using System.ComponentModel;
621 using System.Data;
622 using System.Drawing;
623 using System.Linq;
624 using System.Text;
625 using System.Threading.Tasks;
626 using System.Windows.Forms;
627 using System.IO;
628 private void button10_Click(object sender, EventArgs e)
629 {
630     double x1 = 0, y1 = 0, z1 = 0, x2 = 0, y2 = 0, z2 = 0, d1 = 0, d2 = 0, h1 = 0, h2 = 0;
631     double l = Convert.ToDouble(textBox9.Text);
632     double f = 0, nl = Convert.ToDouble(textBox7.Text);
633     string[] SplitTxt = textBox2.Text.Split(',');
634     for (long i = 0; i < SplitTxt.Length - 9; i += 5)
635     {
636         d1 = Convert.ToDouble(SplitTxt[i + 1]);
637         x1 = Convert.ToDouble(SplitTxt[i + 2]);
638         y1 = Convert.ToDouble(SplitTxt[i + 3]);
639         z1 = Convert.ToDouble(SplitTxt[i + 4]);
640         d2 = Convert.ToDouble(SplitTxt[i + 6]);
641         x2 = Convert.ToDouble(SplitTxt[i + 7]);
642         y2 = Convert.ToDouble(SplitTxt[i + 8]);
643         z2 = Convert.ToDouble(SplitTxt[i + 9]);
644         h1 = z1 - d1;
645         h2 = z2 - d2;
646         l += Math.Sqrt((x1 - x2) * (x1 - x2) + (y1 - y2) * (y1 - y2) + (h1 - h2) * (h1 - h2));
647     }
648     textBox8.Text = l.ToString();
649     f = (nl - l) / nl;
650     ff = f;
651     textBox5.Text = Convert.ToDouble(f).ToString("P");
652 }
653 private void button9_Click(object sender, EventArgs e)
654 {
655     double f1 = ff;
656     double l1 = 0;
657     string zb = ""; string[] SplitTxt = textBox3.Text.Split(',');
658     for (long i = 0; i < SplitTxt.Length - 1; i += 2)
659     {
660         l1 = Convert.ToDouble(SplitTxt[i + 1]);
```

```

661         l1 += (-ff) * l1;
662         double x1 = 0, y1 = 0, z1 = 0, x2 = 0, y2 = 0, z2 = 0, d1 = 0, d2 = 0, h1 = 0, h2 = 0, l0=0,l2=0;
663         double l = Convert.ToDouble(textBox9.Text);
664         double x = 0, y = 0, h = 0;
665         string[] SplitTxt1 = textBox2.Text.Split(',');
666         for (long j = 0; j < SplitTxt1.Length - 9; j += 5)
667         {
668             d1 = Convert.ToDouble(SplitTxt1[j + 1]);
669             x1 = Convert.ToDouble(SplitTxt1[j + 2]);
670             y1 = Convert.ToDouble(SplitTxt1[j + 3]);
671             z1 = Convert.ToDouble(SplitTxt1[j + 4]);
672             d2 = Convert.ToDouble(SplitTxt1[j + 6]);
673             x2 = Convert.ToDouble(SplitTxt1[j + 7]);
674             y2 = Convert.ToDouble(SplitTxt1[j + 8]);
675             z2 = Convert.ToDouble(SplitTxt1[j + 9]);
676             h1 = z1 - d1; h2 = z2 - d2;
677             l0= Math.Sqrt((x1 - x2) * (x1 - x2) + (y1 - y2) * (y1 - y2) + (h1 - h2) * (h1 - h2));
678             l = l + l0;
679             if (l - l1 < 0)
680             {
681                 ;
682             }
683             else if (l - l1 > 0)
684             {
685                 l2 = l0 - (l - l1);
686                 x = x1 + (x2 - x1) * l2 / l0;
687                 y = y1 + (y2 - y1) * l2 / l0;
688                 h = h1 + (h2 - h1) * l2 / l0;
689                 string xx, yy, hh, v;
690                 v = SplitTxt[i];
691                 xx = Convert.ToDouble(x).ToString();
692                 yy = Convert.ToDouble(y).ToString();
693                 hh = Convert.ToDouble(h).ToString();
694                 zb += v + ", " + xx + ", " + yy + ", " + hh + ",\n";
695                 break;
696             }
697         }
698     }
699     textBox6.Text = zb;
700 }

```

Appendix 7 Pipeline Landslide Risk Assessment Results

Fid	Start	Terminus	Susceptibility	Susceptibility level	Vulnerability	Vulnerability level	Risk	Risk level
1	K558	K559+446	0.874	IV	0.168	I	0.147	II
2	K559+446	K563+718	0.874	IV	0.178	I	0.156	II
3	K563+718	K564+883	0.932	IV	0.143	I	0.133	II
4	K564+883	K566+90	0.943	IV	0.149	I	0.141	II
5	K566+90	K567+117	0.943	IV	0.280	II	0.264	III
6	K567+117	K567+224	0.766	IV	0.095	I	0.073	I
7	K567+224	K567+384	0.729	III	0.117	I	0.085	II
8	K567+384	K567+674	0.729	III	0.079	I	0.058	I
9	K567+674	K567+782	0.729	III	0.141	I	0.103	II
10	K567+782	K567+846	0.729	III	0.066	I	0.048	I
11	K567+846	K567+904	0.729	III	0.097	I	0.071	I
12	K568+904	K568+197	0.722	III	0.154	I	0.111	II
13	K568+197	K568+430	0.763	IV	0.144	I	0.110	II
14	K569+430	K569+419	0.739	III	0.186	I	0.137	II
15	K569+419	K569+443	0.739	III	0.141	I	0.104	II
16	K569+443	K569+467	0.739	III	0.107	I	0.079	II
17	K569+467	K569+578	0.739	III	0.121	I	0.089	II
18	K569+578	K569+920	0.739	III	0.107	I	0.079	II
19	K571+920	K571+123	0.736	III	0.127	I	0.093	II
20	K571+123	K571+982	0.799	IV	0.109	I	0.087	II
21	K572+982	K572+729	0.753	IV	0.090	I	0.068	I
22	K573+729	K573+548	0.802	IV	0.094	I	0.075	I
23	K574+548	K574+249	0.805	IV	0.084	I	0.068	I
24	K574+249	K574+525	0.805	IV	0.150	I	0.121	II
25	K575+525	K575+538	0.805	IV	0.115	I	0.093	II
26	K575+538	K575+600	0.805	IV	0.157	I	0.126	II
27	K576+600	K576+737	0.816	IV	0.108	I	0.088	II
28	K577+737	K577+120	0.889	IV	0.089	I	0.079	I
29	K577+120	K577+146	0.889	IV	0.094	I	0.084	I
30	K577+146	K577+187	0.889	IV	0.169	I	0.150	II
31	K578+187	K578+571	0.889	IV	0.118	I	0.105	II
32	K578+571	K578+608	0.889	IV	0.095	I	0.084	I
33	K579+608	K579+624	0.853	IV	0.133	I	0.113	II
34	K580+624	K580+582	0.871	IV	0.156	I	0.136	II
35	K581+582	K581+43	0.871	IV	0.097	I	0.084	I
36	K581+43	K581+273	0.871	IV	0.143	I	0.125	II
37	K581+273	K581+536	0.880	IV	0.125	I	0.110	II
38	K581+536	K581+659	0.872	IV	0.154	I	0.134	II
39	K582+659	K582+263	0.830	IV	0.152	I	0.126	II
40	K582+263	K582+437	0.830	IV	0.116	I	0.096	II
41	K583+437	K583+512	0.830	IV	0.152	I	0.126	II
42	K583+512	K583+693	0.798	IV	0.105	I	0.084	II
43	K583+693	K583+720	0.740	III	0.113	I	0.084	II
44	K585+720	K585+55	0.740	III	0.178	I	0.132	II
45	K585+55	K585+101	0.668	III	0.196	I	0.131	II
46	K585+101	K585+370	0.668	III	0.178	I	0.119	II
47	K585+370	K585+634	0.696	III	0.190	I	0.132	II
48	K585+634	K585+734	0.668	III	0.116	I	0.077	II

49	K585+734	K585+908	0.627	III	0.198	I	0.124 II
50	K585+908	K585+949	0.627	III	0.168	I	0.105 II
51	K586+949	K586+782	0.627	III	0.173	I	0.108 II
52	K586+782	K586+805	0.627	III	0.117	I	0.073 II
53	K587+805	K587+364	0.627	III	0.171	I	0.107 II
54	K587+364	K587+498	0.618	III	0.078	I	0.048 I
55	K587+498	K587+794	0.618	III	0.107	I	0.066 I
56	K589+794	K589+251	0.618	III	0.102	I	0.063 I
57	K590+251	K590+757	0.618	III	0.172	I	0.106 II
58	K590+757	K590+780	0.556	III	0.153	I	0.085 II
59	K590+780	K590+812	0.556	III	0.123	I	0.068 II
60	K591+812	K591+500	0.555	III	0.135	I	0.075 II
61	K591+500	K591+946	0.555	III	0.087	I	0.048 I
62	K592+946	K592+259	0.555	III	0.107	I	0.059 I
63	K593+259	K593+631	0.517	III	0.152	I	0.079 II
64	K593+631	K593+912	0.374	II	0.153	I	0.057 II
65	K594+912	K594+993	0.374	II	0.150	I	0.056 II
66	K595+993	K595+203	0.374	II	0.076	I	0.028 I
67	K595+203	K595+261	0.359	II	0.114	I	0.041 I
68	K595+261	K595+383	0.359	II	0.099	I	0.036 I
69	K596+383	K596+383	0.412	II	0.278	II	0.115 II
70	K596+383	K596+429	0.412	II	0.107	I	0.044 I
71	K597+429	K597+62	0.359	II	0.121	I	0.043 I
72	K597+62	K597+200	0.412	II	0.158	I	0.065 II
73	K597+200	K597+345	0.412	II	0.133	I	0.055 I
74	K597+345	K597+680	0.412	II	0.273	II	0.112 II
75	K599+680	K599+376	0.321	II	0.461	II	0.148 II
76	K599+376	K599+693	0.211	I	0.105	I	0.022 I
77	K600+693	K600+188	0.211	I	0.179	I	0.038 I
78	K600+188	K600+353	0.106	I	0.172	I	0.018 I
79	K601+353	K601+369	0.106	I	0.264	II	0.028 I
80	K602+369	K602+495	0.099	I	0.190	I	0.019 I
81	K603+495	K603+131	0.067	I	0.436	II	0.029 I
82	K603+131	K603+551	0.099	I	0.144	I	0.014 I
83	K604+551	K604+321	0.104	I	0.253	II	0.026 I
84	K604+321	K604+976	0.099	I	0.102	I	0.010 I
85	K605+976	K605+735	0.178	I	0.372	II	0.066 II
86	K606+735	K606+368	0.236	I	0.637	III	0.150 II
87	K606+368	K606+838	0.236	I	0.127	I	0.030 I
88	K607+838	K607+596	0.323	II	0.407	II	0.131 II
89	K608+596	K608+20	0.323	II	0.163	I	0.053 II
90	K608+20	K608+287	0.323	II	0.145	I	0.047 I
91	K608+287	K608+546	0.346	II	0.084	I	0.029 I
92	K608+546	K608+583	0.406	II	0.215	I	0.087 II
93	K608+583	K608+835	0.406	II	0.291	II	0.118 II
94	K609+835	K609+565	0.442	II	0.279	II	0.123 II
95	K610+565	K610+564	0.442	II	0.403	II	0.178 II
96	K610+564	K610+945	0.442	II	0.453	II	0.200 II
97	K611+945	K611+89	0.482	II	0.117	I	0.056 I
98	K611+89	K611+691	0.501	III	0.138	I	0.069 II
99	K612+691	K612+413	0.501	III	0.175	I	0.088 II

100	K613+413	K613+269	0.501	III	0.163	I	0.082	II
101	K613+269	K613+442	0.502	III	0.166	I	0.083	II
102	K614+442	K614+83	0.502	III	0.354	II	0.178	II
103	K614+83	K614+980	0.502	III	0.263	II	0.132	II
104	K615+980	K615+218	0.601	III	0.153	I	0.092	II
105	K615+218	K615+388	0.601	III	0.143	I	0.086	II
106	K616+388	K616+87	0.635	III	0.126	I	0.080	II
107	K616+87	K616+300	0.556	III	0.144	I	0.080	II
108	K616+300	K616+460	0.505	III	0.269	II	0.136	II
109	K617+460	K617+715	0.505	III	0.172	I	0.087	II
110	K617+715	K617+827	0.505	III	0.255	II	0.129	II
111	K618+827	K618+28	0.556	III	0.170	I	0.095	II
112	K618+28	K618+687	0.556	III	0.313	II	0.174	II
113	K620+687	K620+78	0.556	III	0.188	I	0.105	II
114	K620+78	K620+298	0.425	II	0.196	I	0.083	II
115	K621+298	K621+509	0.576	III	0.223	I	0.128	II
116	K621+509	K621+611	0.425	II	0.107	I	0.045	I
117	K622+611	K622+10	0.425	II	0.262	II	0.111	II
118	K622+10	K622+86	0.425	II	0.122	I	0.052	I
119	K622+86	K622+539	0.693	III	0.178	I	0.123	II
120	K622+539	K622+897	0.634	III	0.549	III	0.348	III
121	K623+897	K623+36	0.634	III	0.535	III	0.339	III
122	K623+36	K623+794	0.693	III	0.145	I	0.100	II
123	K624+794	K624+866	0.693	III	0.310	II	0.215	II
124	K625+866	K625+242	0.796	IV	0.137	I	0.109	II
125	K627+242	K627+60	0.859	IV	0.452	II	0.388	III
126	K627+60	K627+162	0.859	IV	0.193	I	0.166	II
127	K627+162	K627+313	0.859	IV	0.166	I	0.143	II
128	K627+313	K627+700	0.783	IV	0.167	I	0.131	II
129	K628+700	K628+146	0.908	IV	0.501	III	0.455	III
130	K628+146	K628+196	0.908	IV	0.139	I	0.126	II
131	K628+196	K628+610	0.908	IV	0.631	III	0.573	IV
132	K629+610	K629+355	0.787	IV	0.369	II	0.290	III
133	K629+355	K629+525	0.787	IV	0.729	III	0.574	IV
134	K629+525	K629+570	0.787	IV	0.252	II	0.198	II
135	K629+570	K629+620	0.787	IV	0.465	II	0.366	III
136	K630+620	K630+348	0.787	IV	0.286	II	0.225	II
137	K630+348	K630+956	0.892	IV	0.389	II	0.347	III
138	K631+956	K631+116	0.886	IV	0.423	II	0.375	III
139	K631+116	K631+528	0.805	IV	0.513	III	0.413	III
140	K633+528	K633+435	0.805	IV	0.568	III	0.457	III
141	K635+435	K635+302	0.933	IV	0.625	III	0.583	IV
142	K635+302	K635+326	0.884	IV	0.611	III	0.540	III
143	K635+326	K635+359	0.884	IV	0.441	II	0.390	III
144	K635+359	K635+368	0.884	IV	0.194	I	0.171	II
145	K635+368	K635+530	0.884	IV	0.374	II	0.331	III
146	K635+530	K635+604	0.884	IV	0.307	II	0.271	III
147	K635+604	K635+850	0.805	IV	0.377	II	0.303	III
148	K635+850	K635+943	0.805	IV	0.234	I	0.188	II
149	K635+943	K635+972	0.805	IV	0.139	I	0.112	II
150	K635+972	K635+974	0.805	IV	0.121	I	0.097	II

151	K635+974	K635+990	0.805	IV	0.138	I	0.111 II
152	K636+990	K636+152	0.933	IV	0.598	III	0.558 III
153	K636+152	K636+159	0.933	IV	0.157	I	0.146 II
154	K636+159	K636+320	0.884	IV	0.579	III	0.512 III
155	K636+320	K636+427	0.884	IV	0.166	I	0.147 II
156	K636+427	K636+517	0.884	IV	0.124	I	0.110 II
157	K636+517	K636+806	0.834	IV	0.663	III	0.553 III
158	K636+806	K636+893	0.834	IV	0.794	IV	0.662 IV
159	K637+893	K637+57	0.834	IV	0.519	III	0.433 III
160	K637+57	K637+109	0.834	IV	0.542	III	0.452 III
161	K637+109	K637+181	0.834	IV	0.111	I	0.093 II
162	K637+181	K637+332	0.834	IV	0.127	I	0.106 II
163	K638+332	K638+87	0.834	IV	0.608	III	0.507 III
164	K638+87	K638+140	0.834	IV	0.157	I	0.131 II
165	K638+140	K638+193	0.767	IV	0.682	III	0.523 III
166	K638+193	K638+199	0.767	IV	0.188	I	0.144 II
167	K638+199	K638+226	0.767	IV	0.126	I	0.097 II
168	K638+226	K638+368	0.767	IV	0.532	III	0.408 III
169	K638+368	K638+409	0.767	IV	0.604	III	0.463 III
170	K638+409	K638+432	0.767	IV	0.205	I	0.157 II
171	K638+432	K638+444	0.767	IV	0.525	III	0.403 III
172	K638+444	K638+676	0.767	IV	0.173	I	0.133 II
173	K638+676	K638+837	0.767	IV	0.479	II	0.367 III
174	K639+837	K639+266	0.744	III	0.483	II	0.359 III
175	K639+266	K639+339	0.744	III	0.427	II	0.318 III
176	K639+339	K639+435	0.744	III	0.549	III	0.408 III
177	K639+435	K639+562	0.631	III	0.324	II	0.204 II
178	K640+562	K640+63	0.607	III	0.476	II	0.289 III
179	K641+63	K641+600	0.607	III	0.604	III	0.367 III
180	K642+600	K642+225	0.607	III	0.461	II	0.280 III

702

703

704

Appendix 8 Field environment of study area



705

706

Figure 1 Vegetation distribution in a watershed of the study area



707

708

Figure 2 Vegetation environment of a pipeline section in the study area



709

710

Figure 3 Outcropping of rock strata in the study area